Receptor-Based Mechanism of Relative Sensing in Mammalian Signaling Networks

Eugenia Lyashenko[1□], Mario Niepel[2□], Purushottam Dixit[1□], Sang Kyun Lim[2], Peter K. Sorger[2] & Dennis Vitkup[1,3,*]

[1]Department of Systems Biology, Center for Computational Biology and Bioinformatics, Columbia University, New York, New York, USA. [2]Department of Systems Biology, Harvard Medical School, Boston, MA. [3]Department of Biomedical Informatics, Columbia University, New York, New York, USA. [□]Equal Contributors

*correspondence to DV at dv2121@columbia.edu

Abstract

Mammalian cells operate in fluctuating environments by perceiving and reacting to a diverse set of extracellular stimuli[1]. Detecting relative rather than absolute changes in their environments may enable cells to make decisions in diverse biological contexts[2, 3]. However, precise molecular mechanisms underlying such relative sensing by mammalian signaling networks are not well understood. Here we use a combined computational and experimental analysis to investigate the growth factor activated immediate-early phosphorylation response of protein kinase B (Akt). We demonstrate that activity-dependent receptor degradation allows cells to robustly detect fold changes in extracellular Epidermal Growth Factor (EGF) levels across orders of magnitude of EGF background concentrations. Interestingly, we show that the memory of the background stimulation is effectively encoded in the number of EGF receptors on the cell surface. We further demonstrate that the ability to sense relative changes by the Akt pathway extends to hepatocyte growth factor (HGF) signaling. We develop an analytical model that reveals key aggregate network parameters controlling the relative sensing capabilities of the system. The mechanism described in our study could play a role in multiple other sensory cascades where stimulation leads to a proportional reduction in the abundance of cell surface receptors. Beyond simple receptor and signal downregulation, this mechanism may allow cells to continuously monitor their environments and store the memory of past ligand exposures.

Stimulation of mammalian cells with growth factors elicits a variety of context-dependent phenotypic responses, including cell migration, proliferation, and cell survival[1]. One of the central hubs in growth factor signaling cascades, protein kinase B (Akt)[4] is a key regulator of cellular decision processes. Concomitant with its importance in cell signaling, Akt phosphorylation-dependent pathways are implicated in multiple human diseases, such as many types of cancers[4, 5], diabetes[6] and psychiatric disorders[7, 8].

To understand how the immediate-early dynamics of the EGFR/Akt pathway depends on the background level of EGF we used immunofluorescence to quantify the pAkt signal in human non-transformed mammary epithelial MCF10A cells (SI section II). In agreement with previous studies[9], upon continuous stimulation with EGF, pAkt reached maximum response within minutes of EGF exposure and then decayed to very low levels within hours (Figure 1a). Notably, in the sensitive range of EGF concentrations, maximal pAkt response depended approximately on the logarithm of the EGF stimulus (Figure 1b). As a result of continuous stimulation with EGF, the abundance of cell-surface EGFR (sEGFR) decreased proportionally to the logarithm of the background EGF level and reached a new steady state within hours (Figure 1c). Prior exposure with EGF desensitized cells to subsequent EGF stimulations in a quantitative manner, i.e. maximal pAkt response to the same EGF stimulation (2 ng/ml) was monotonically attenuated with increasing pre-exposure EGF levels (Figure 1d). These results suggest that the strength of the pAkt responses to EGF stimulation is modulated by background EGF levels and that this effect is mediated by the removal of activated EGFRs from cell surface[10].

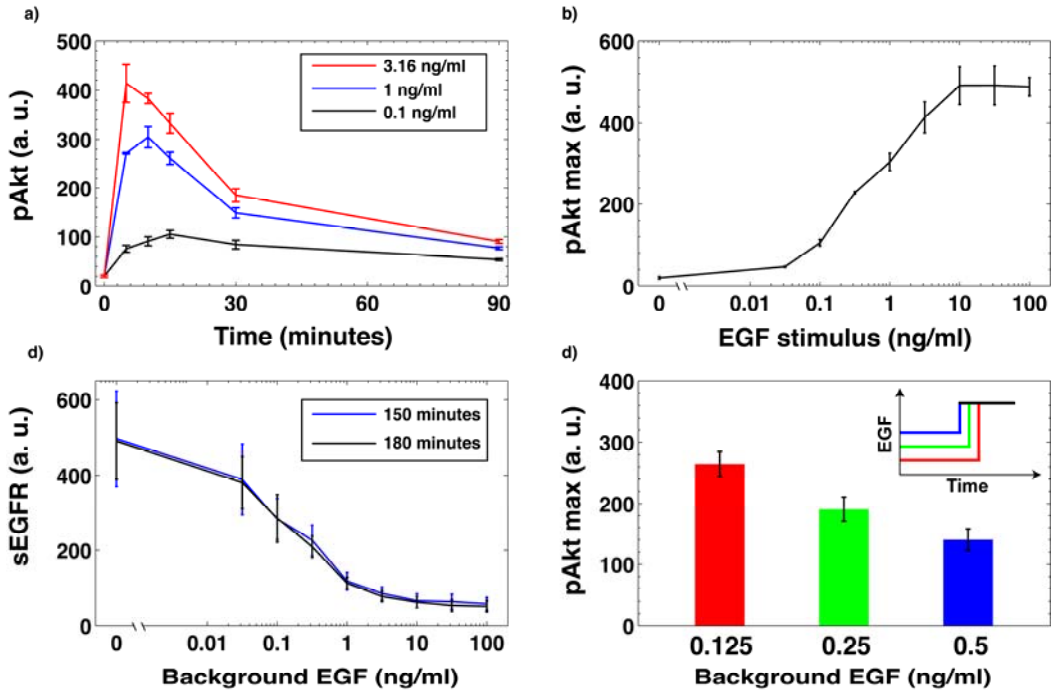

Figure 1: EGF-activated Akt phosphorylation and desensitization. (a) Time-dependent levels of phosphorylated Akt (pAkt) in MCF10A cells exposed to increasing stimulation with extracellular EGF. (b) Maximal pAkt response as a function of EGF stimulus. (c) Steady state levels of surface EGFR (sEGFR) after 150 and 180 minutes of stimulation with a constant dose of EGF. (d) Desensitization of the maximal pAkt response. In three different experiments (represented by bars and inset curves with different colors) MCF10A cells were pre-treated with increasing background doses of EGF for three hours, followed by the second stimulation with 2 ng/ml of EGF. Error bars represent the standard deviation of technical replicates.

To understand how the background EGF levels affect pAkt response to subsequent EGF stimulation we constructed an ordinary differential equation (ODE) model of EGF-dependent Akt phosphorylation. Following our previous work[9] (SI section III), the model included several well-established features of the EGFR signaling cascade, such as ligand-receptors interactions, receptor dimerization[11], phosphorylation and de-phosphorylation of receptors[12], receptor endocytosis[10, 13], recycling[14], and degradation[10] (Figure 2a). We constrained the ranges of model parameters based on literature-derived estimates (SI Table 1), and fitted the model using pAkt time courses and steady state sEGFR levels at different doses of EGF stimulations. Parameter optimization was performed using simulated annealing (SA)[15] (SI section III). Parameters of ODE models describing complex signaling networks are usually underdetermined with multiple distinct parameter sets producing similar fits to the data[16]. Therefore, we considered multiple distinct parameter sets obtained from the optimization runs for further computational analysis and model predictions (SI Figure 8a, b).

Using the fitted dynamical model, we explored the possibility of quantitative relative sensing in the network, i.e. the ability of the Akt pathway to respond to relative, rather than absolute, changes in EGF levels. To that end, we simulated pAkt response by exposing the model *in silico* to a range of background EGF levels and then, after the system reached the background-dependent steady state, we simulated different fold change increases in EGF concentration (Figure 2b). The model predicted that the maximal pAkt response after the step change in EGF concentration indeed depends primarily on the EGF fold change relative to the background stimulation (Figure 2c). The relative sensing occurred over an order of magnitude of background EGF concentrations and the resulting pAkt response was approximately proportional to the logarithm of the EGF fold change (Figure 2d). Importantly, the model predicted relative sensing in the range of EGF background concentrations where endocytosis was sensitive to the background ligand stimulation. At low EGF background concentrations (< 0.01 ng/ml), no substantial sEGFR removal was predicted at steady state (SI Figure 8b), and consequently there was no significant desensitization of the pAkt response. In that regime the pAkt response after a step change depended primarily on the absolute EGF level. On the other hand, at high background EGF concentrations (> 1 ng/ml), a large fraction of sEGFR was removed from cell surface and consequently the network responded only weakly to further EGF stimulation.

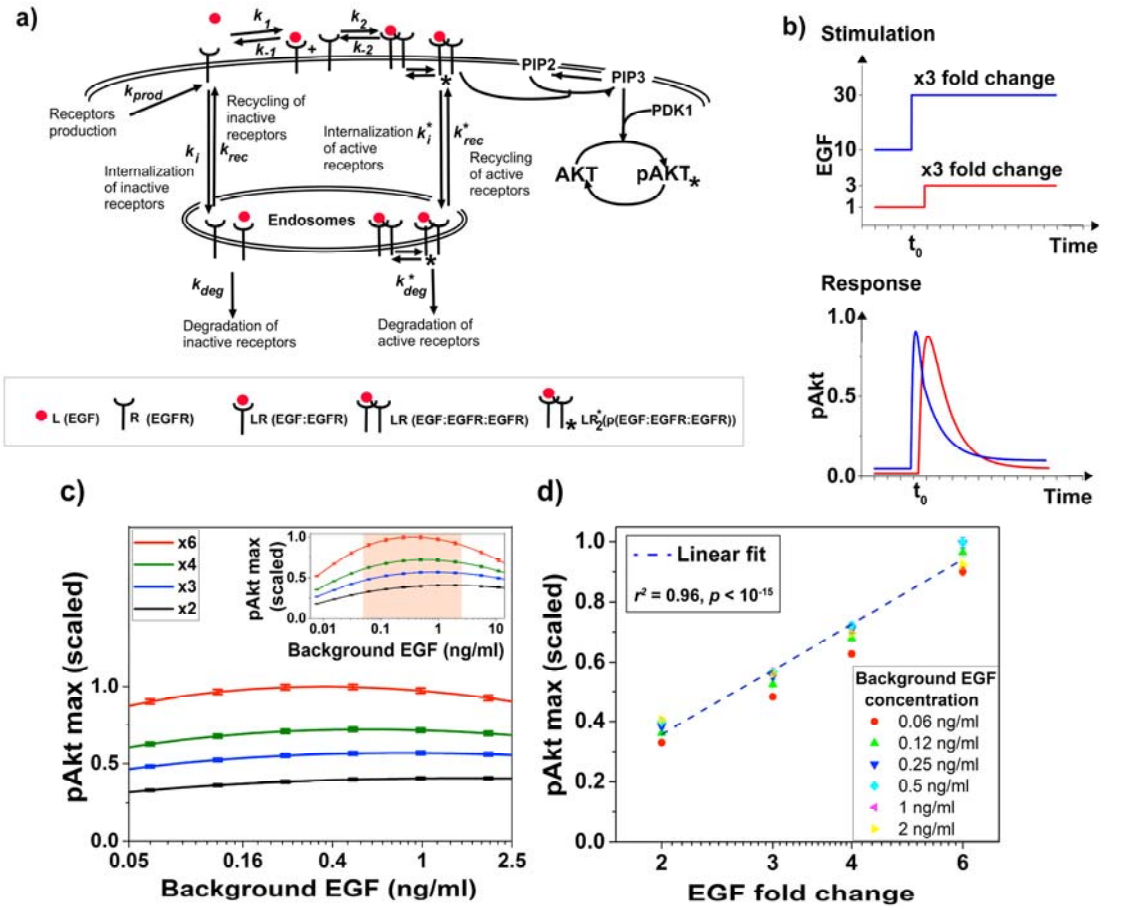

Figure 2: Computational model predicts pAkt sensing of relative changes in EGF levels. (a) Computational model of the EGF-induced EGFR signaling leading to phosphorylation of Akt. Phosphorylated receptors are referred to as activated and unphosphorylated receptors are referred to as non-activated; rate constants with asterisks refer to reactions related to activated receptors. Only a subset of key reactions in the network are shown for brevity. (b) Illustration of the protocol used to explore relative sensing, showing EGF stimulation (top) and the corresponding pAkt response (bottom). In this example, cells first exposed to different background EGF stimulations (blue and red) were next subjected to the same 3-fold change in EGF at time t_0 and the resulting maximal pAkt responses were similar, thus indicating relative sensing. (c) The ODE model prediction of relative sensing by pAkt. The maximal pAkt response observed after exposing the model *in silico* to different background EGF levels (x axis), followed by a 2-, 3-, 4-, or 6- fold increase (different colors) of EGF; inset shows pAkt response over a wider range of background EGF levels. (d) Maximum pAkt responses from stimulations with various EGF background levels (indicated by data points with the same shape and color) were combined and plotted as a function of the fold change in EGF dose (x axis). Dashed line represents log-linear fit to data (Pearson's $r^2 = 0.96$, $p < 10^{-15}$). Error bars represent the standard deviation of top 10 model fits.

Following the computational analysis, we experimentally tested the model-predicted relative sensing behavior in MCF10A cells. Cells were first treated with various background EGF stimulations for three hours to ensure that steady state sEGFR levels were reached and that pAkt decayed after a transient increase (Figure 1c). Similar to the

protocol used in the computational analysis (Figure 2b), cells were then exposed to different fold changes in EGF levels. To determine the maximum pAkt response after the fold change, pAkt levels were measured over the course of 45 minutes (at 2.5, 5, 10, 15, 30 and 45 minutes) after the step increase in EGF stimulation (SI Figure 1a, b); similar results were obtained in two independent biological replicates (Pearson's r^2 = 0.94, $p < 10^{-5}$, SI Figures 3 and 4a, b). The experiments confirmed that the maximum pAkt response indeed depended primarily on the fold change in EGF levels and not its absolute concentration (Figure 3a, SI Figure 2). Specifically, across more than an order of magnitude of EGF background concentrations (0.03 - 0.5 ng/ml) the same EGF fold change, indicated by lines of the same colors in Figure 3a, elicited similar pAkt responses. Moreover, in good agreement with model predictions, when considered across different background EGF concentrations, the maximum pAkt response was approximately proportional to the logarithm of EGF fold change (Figure 3b).

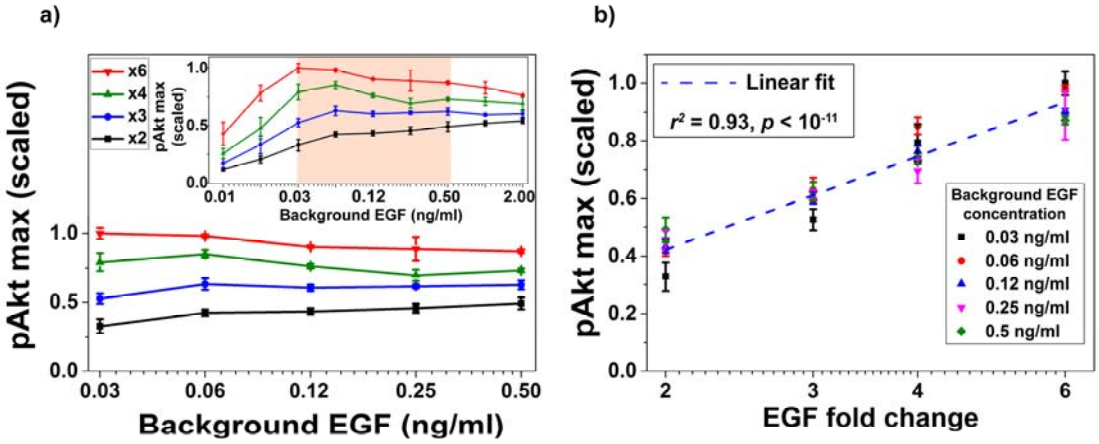

Figure 3: Experimental confirmation of relative sensing of extracellular EGF levels by pAkt. (a) The maximum pAkt responses after exposing MCF10A cells to different background EGF levels (x axis) for 3 hours followed by 2-, 3-, 4-, and 6-fold increase (different colors) of EGF. Inset shows experimental pAkt response over a wider range of background EGF levels. (b) Confirming computational predictions, maximum pAkt responses to fold changes in EGF depended approximately logarithmically on the fold change. Maximum pAkt responses from experiments with various EGF background levels (indicated by data points with the same shape and color) were combined and plotted as a function of the fold change in EGF dose (x axis). Dashed line represents log-linear fit to the data (Pearson's r^2 = 0.93, $p < 10^{-11}$). Error bars represent the standard deviation of technical replicates.

To better understand the molecular mechanism responsible for the observed relative sensing of extracellular EGF concentration, next we constructed a simplified analytical model focused on the receptor level of the signaling network (SI section IV). The model revealed that across a broad range of background stimulations the steady-

state abundance of cell surface receptors $[R]_T$ decreases approximately log-linearly as a function of the background ligand (EGF) concentration $[L]_0$ (Equation 1 and Figure 4a)

$$[R]_T \sim constant - a * \log[L]_0 \quad (1)$$

and that the maximal receptors phosphorylation response $[LR^*_2]$ depends approximately log-linearly on the level of the subsequent stimulation $[L]_1$ and linearly on the steady-state receptor abundance $[R]_T$ (Equation 2, Figure 4b),

$$[LR_2^*] \sim b * \left(\log[L]_1 + \frac{[R]_T}{a}\right) + constant \quad (2)$$

where *a* and *b* are numerical constants (SI section IV). As a result of these relationships, the phosphorylation response $[LR^*_2]$ after an increase in ligand concentration from $[L]_0$ to $[L]_1$ depends, in agreement with computational and experimental analyses, approximately on the logarithm of the stimulation fold change $[L]_1/[L]_0$ (SI section IV):

$$[LR_2^*] \sim b * \left(\log[L]_1 + \frac{[R]_T}{a}\right) \sim b * (\log[L]_1 - \log[L]_0) \sim b * \log\frac{[L]_1}{[L]_0} \quad (3)$$

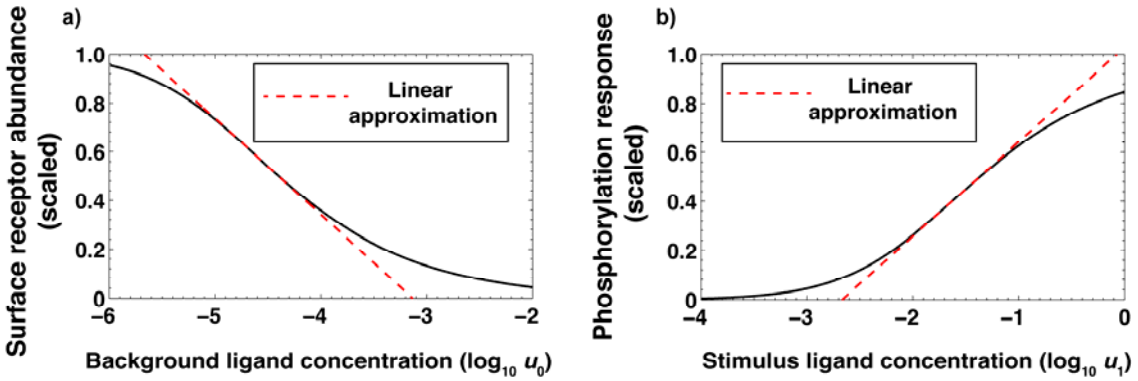

Figure 4: Analytical model reveals the mechanism of relative sensing. (a) Approximate log-linear dependence of the scaled steady-state receptor abundance $[R]_T$ on the normalized background ligand concentration $u_0 = [L]_0/K_{d1}$, where K_{d1} is the equilibrium dissociation constant of EGF binding to EGFR. (b) Approximate log-linear dependence of the maximum phosphorylation response on the normalized ligand stimulus $u_1 = [L]_1/K_{d1}$. Dashed red lines represent the log-linear approximation.

The analytical model also revealed that the range of the background ligand concentrations where the relative sensing is observed is primarily determined by two aggregate parameters, which we denote α and β (Equations 4 and 5). Intuitively, the parameter α quantifies the ability of the signaling system to capture the signal (EGF) and elicit a phosphorylation response, while the parameter β quantifies the ability of the system to preferentially internalize and degrade active (phosphorylated) receptors compared to inactive (non-phosphorylated) receptors. The two aggregate parameters are expressed as follows:

$$\alpha = \frac{k_p + k_{dp}}{k_{dp}} \times \frac{k_2}{k_{-2}} \times R_0 \tag{4}$$

where k_p is the rate of receptor phosphorylation and k_{dp} is the rate of receptor de-phosphorylation, k_2 is the rate of receptor dimerization, k_{-2} is the rate of dissociation of receptor dimers, and R_0 is the total number of cell-surface receptors at steady state in the absence of extracellular stimuli.

$$\beta = \frac{k_p}{k_{dp} + k_p} \times \frac{k_i^*}{k_i} \times \frac{\frac{k_{deg}^*}{k_{deg}^* + k_{rec}^*}}{\frac{k_{deg}}{k_{deg} + k_{rec}}} \tag{5}$$

where k_i^*, k_{rec}^*, k_{deg}^* and k_i, k_{rec}, k_{deg} are correspondingly the rates of internalization, recycling and degradation of the active and non-active receptors. An increase in the value of α leads to a higher signal sensitivity and an increase in receptor dimerization and phosphorylation. This shifts the relative sensing range to lower ligand concentrations. In turn, an increase in the value of β leads to a larger fraction of active (phosphorylated) receptors being internalized and degraded. This generally increases the range of background signal concentrations where the relative sensing is observed. Based on the best-fit ODE model parameter sets, we estimate α ~ 25 and β ~ 1000 (SI section IV). As an example, in Figure 5 we show the scaled phosphorylation response following a six-fold increase in EGF concentration as a function of the background concentration $[L]_0$ for different values of parameters α (Figure 5a) and β (Figure 5b); the colors in the figure represent different accuracy ranges of relative sensing; the horizontal green arrows represent the predicted range of relative sensing of the EGF/EGFR system. The model demonstrates that the relative sensing generally occurs across over an order of magnitude of background ligand concentrations.

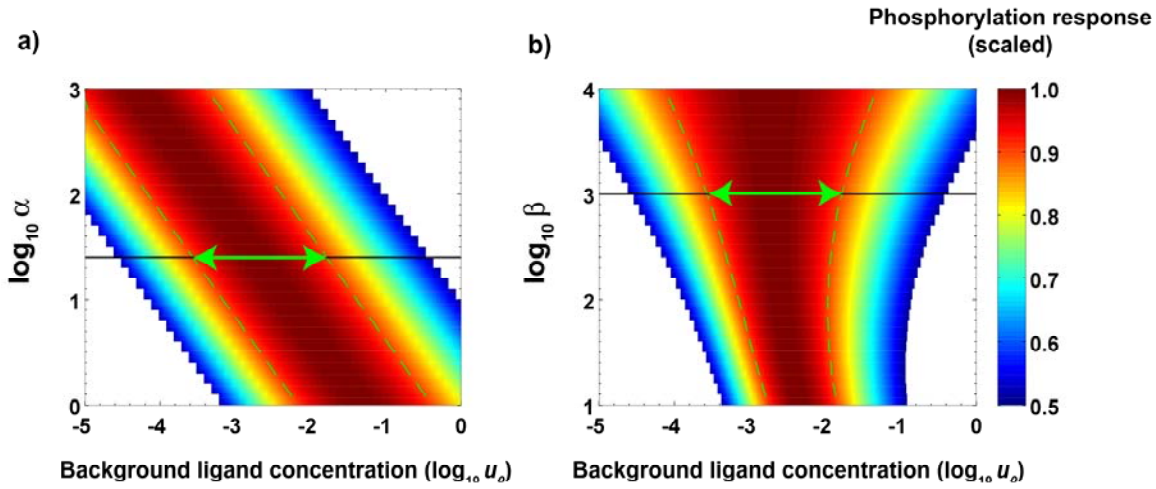

Figure 5: Analytical model predictions of the range and accuracy of relative sensing. As an example, the predicted phosphorylation response after a 6-fold change in extracellular EGF is shown in the figure. The colors represent the predicted accuracy ranges of relative sensing. Specifically, the green dashed lines show the range of background concentrations where the scaled response is within 90% of the maximum. (a) Dependence of the phosphorylation response [LR^*_2] after a 6-fold change in extracellular EGF on the normalized background ligand concentrations $u_0 = [L]_0/K_{d1}$ at different values of α when $\beta = 1000$. (b) Dependence of the phosphorylation response after a 6-fold change in extracellular EGF on normalized background ligand concentrations at different values of β when $\alpha = 25$. The horizontal green arrows represent the predicted range of relative sensing calculated from model-derived EGF/EGFR parameter values.

In addition to EGF, Akt phosphorylation can be induced by multiple other ligands, including hepatocyte growth factor (HGF)[17] which binds to its cognate receptor cMet[18]. EGF- and HGF-induced Akt phosphorylation cascades share most of their components downstream of their cognate receptors[19]. Therefore, we explored next how specific is the memory of past ligand exposure to cell surface abundance of the ligand-cognate receptors. We exposed cells to various background doses of either HGF or EGF for three hours, and then stimulated cells using either the same or the other growth factor and measured pAkt levels 10 minutes after the addition of the second stimulus (Figure 6). Pre-exposure with HGF did not substantially downregulate EGF-induced pAkt responses, but substantially decreased HGF-induced responses (Figure 6a). Similarly, there was a relatively small desensitization of HGF responses due to pre-exposure with EGF, while a significant desensitization of EGF-induced pAkt responses was observed (Figure 6b). We further confirmed that exposure of MCF10A cells to various doses of HGF leads to pronounced HGF-dependent removal of cMet from the cell surface, without significant removal of sEGFR (SI Figure 5a). Similarly, the pre-exposure of cells to EGF leads to EGF-dependent removal of sEGFR without a significant change in

surface cMet abundance (SI Figure 5b). These observations support the mechanism in which the relative sensing of extracellular ligands relies on the memory of their past exposures encoded primarily in the abundances of their cognate cell-surface receptors.

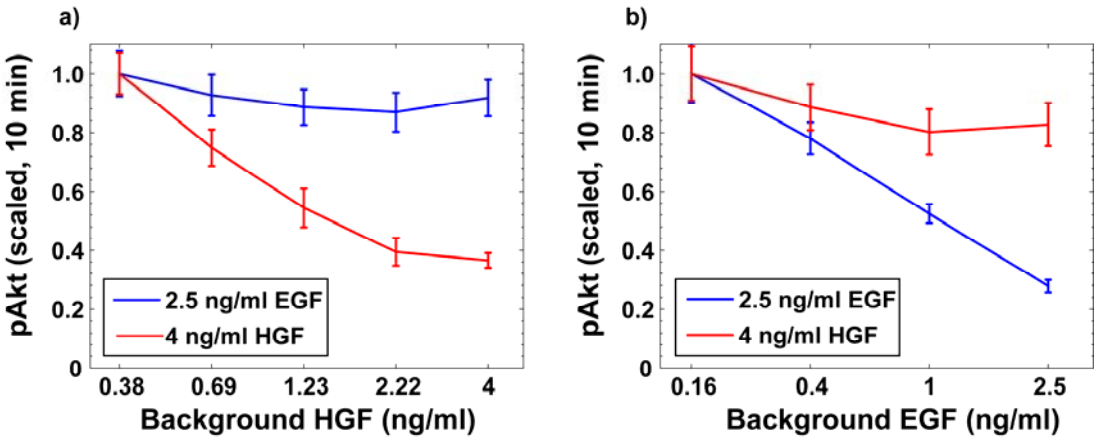

Figure 6: Desensitization of ligand-induced pAkt response depends on the identity of the background ligand. MCF10A cells were exposed to various background doses of either HGF or EGF for three hours, and then stimulated using either the same or the other growth factor. pAkt levels were then measured 10 minutes after the addition of the second stimulus. (a) EGF (blue, 2.5 ng/ml) or HGF (red, 4 ng/ml) induced pAkt response in cells pre-exposed with various doses of HGF (shown on the x-axis) for three hours. (b) EGF (blue, 2.5 ng/ml) or HGF (red, 4 ng/ml) induced pAkt response in cells pre-exposed with various doses of EGF for three hours. Error bars represent the standard deviation of technical replicates.

Given the observed HGF-dependent removal of cell surface cMet receptors and resulting pAkt desensitization, we investigated whether the maximum pAkt response depends, similarly to EGF, on the relative fold changes in the level of extracellular HGF. As in the EGF experiments, we stimulated cells with a range of different background levels of HGF, and then exposed cells to different fold changes in HGF concentrations (Figure 7 and SI Figure 6). These experiments demonstrated that HGF-induced phosphorylation of Akt also depends primarily to the fold changes in extracellular HGF concentrations across almost an order of magnitude of background HGF exposures (between 0.1 and 1 ng/ml HGF) and can distinguish up to 8 fold changes in HGF concentrations (Figure 7a). Moreover, similar to EGF, the maximum pAkt levels depended approximately log-linearly on the fold changes in HGF (Figure 7b).

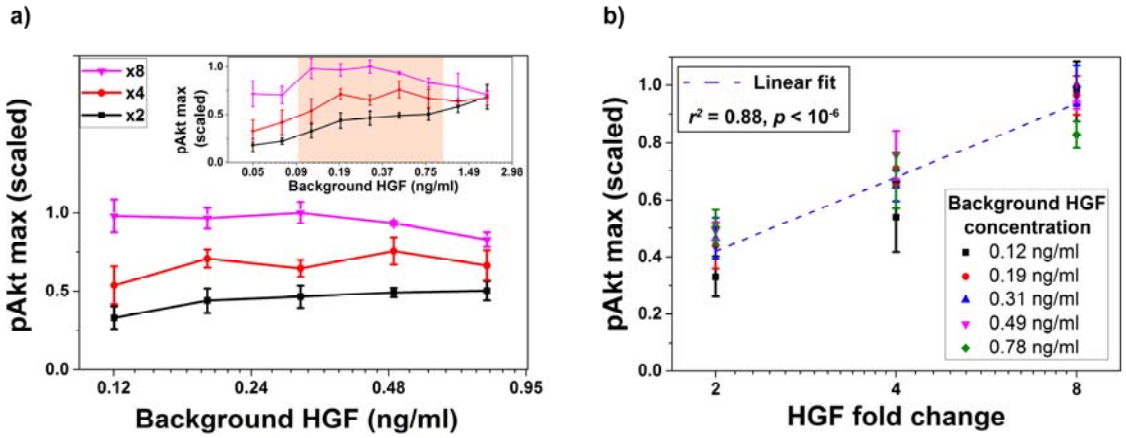

Figure 7: **Relative sensing of extracellular levels of HGF by pAkt.** (a) The maximum pAkt response in MCF10A cells exposed to different background doses of HGF(x-axis) for 3 hours followed by 2-, 4-, and 8-fold increase (different colors) of HGF. Inset shows experimental pAkt response over a wider range of background HGF levels. (b) Similar to EGF, the maximum pAkt responses to HGF fold changes depended approximately logarithmically on the fold change. Maximum pAkt responses from experiments with various HGF background levels (indicated by data points with the same shape and color) were combined and plotted as a function of the fold change in HGF dose (x axis). Dashed line represents log-linear fit to data (Pearson's r^2 = 0.88, p < 10^{-6}). Error bars represent the standard deviation of technical replicates.

The non-transcriptional receptor-based mechanism of relative sensing explored in our paper operates on the time scales of several minutes to hours. In the paper we used the maximal level of pAkt to demonstrate the relative sensing capabilities of the network. Notably, additional experimental and computational analyses show that relative sensing is also observed for the downstream signal defined as the time integral of pAkt levels (SI Figure 7). We further analytically demonstrated that relative sensing does not depend on the receptor dimerization, and that a similar mechanism can function in a pathway where a signal is initiated by monomeric receptors (SI section IV). Receptor endocytosis and downregulation following ligand stimulation has been canonically associated with signal desensitization[20]. Our analysis suggests a more quantitative role for receptors downregulation. Specifically, it may allow cells to continuously monitor signals in their environments[21] and respond to relative changes in environmental stimuli. We note that signal downregulation and adaptation do not always result in relative sensing[22], and our analysis reveals the ranges of network parameters over which relative sensing may occur. Elegant recent studies[23-25] demonstrated that transcriptional motifs may efficiently buffer cell-to-cell variability in signaling components when responding to the same stimulation. In contrast, our study describes a non-transcriptional mechanism of sensing changes relative to past extracellular stimulation.

These two processes are likely to be complementary, thus allowing cells to sense, across different timescales, relative changes in environmental signals while also buffering cellular variability.

Our work may shed light on important design principles of receptor-based signaling systems. Although there are usually ~10^5-10^6 EGFR receptors on mammalian cell surface[26], as was noted previously, the downstream network response, for example Akt phosphorylation, often saturates when only a relatively small fraction (5-10%) of the receptors are bound to their cognate ligands[9, 26]. Our study suggests that one potential advantage of such a system architecture is that, beyond simple signal activation, it may endow cells with a large dynamic range of receptor abundances to memorize stimulation levels of multiple extracellular ligands[27-29]. Signal-mediated removal has been reported for many other receptors and membrane proteins, such as the G protein coupled receptors (GPCRs)[30] involved in multiple sensory systems and AMPA-type glutamate receptors[31, 32] implicated in synaptic plasticity. Therefore, similar relative sensing mechanisms may be important in multiple other receptor-based signaling cascades and different biological contexts.

References

1. Cantley, L.C.H., T. Sever, R. Thorner, J. Signal transduction: principles, pathways, and processes. *Cold Spring Harbor Laboratory Press* (2014).
2. Shoval, O. et al. Fold-change detection and scalar symmetry of sensory input fields. *Proc Natl Acad Sci U S A* **107**, 15995-16000 (2010).
3. Ferrell, J.E., Jr. Signaling motifs and Weber's law. *Mol. Cell* **36**, 724-727 (2009).
4. Hemmings, B.A. & Restuccia, D.F. The PI3K-PKB/Akt pathway. *Cold Spring Harb. Perspect. Biol.* **7** (2015).
5. Engelman, J.A. Targeting PI3K signalling in cancer: opportunities, challenges and limitations. *Nat. Rev. Cancer* **9**, 550-562 (2009).
6. Whiteman, E.L., Cho, H. & Birnbaum, M.J. Role of Akt/protein kinase B in metabolism. *Trends Endocrinol. Metab.* **13**, 444-451 (2002).
7. McGuire, J.L. et al. Altered serine/threonine kinase activity in schizophrenia. *Brain Res.* **1568**, 42-54 (2014).
8. Gilman, S.R. et al. Diverse types of genetic variation converge on functional gene networks involved in schizophrenia. *Nat. Neurosci.* **15**, 1723-1728 (2012).
9. Chen, W.W. et al. Input-output behavior of ErbB signaling pathways as revealed by a mass action model trained against dynamic data. *Mol. Syst. Biol.* **5**, 239 (2009).
10. Wiley, H.S. et al. The role of tyrosine kinase activity in endocytosis, compartmentation, and down-regulation of the epidermal growth factor receptor. *J. Biol. Chem.* **266**, 11083-11094 (1991).

11. Bessman, N.J., Bagchi, A., Ferguson, K.M. & Lemmon, M.A. Complex relationship between ligand binding and dimerization in the epidermal growth factor receptor. *Cell Rep.* **9**, 1306-1317 (2014).
12. Kleiman, L.B., Maiwald, T., Conzelmann, H., Lauffenburger, D.A. & Sorger, P.K. Rapid phospho-turnover by receptor tyrosine kinases impacts downstream signaling and drug binding. *Mol. Cell* **43**, 723-737 (2011).
13. Wiley, H.S. & Cunningham, D.D. The endocytotic rate constant. A cellular parameter for quantitating receptor-mediated endocytosis. *J. Biol. Chem.* **257**, 4222-4229 (1982).
14. Herbst, J.J., Opresko, L.K., Walsh, B.J., Lauffenburger, D.A. & Wiley, H.S. Regulation of postendocytic trafficking of the epidermal growth factor receptor through endosomal retention. *J. Biol. Chem.* **269**, 12865-12873 (1994).
15. Kirkpatrick, S., Gelatt, C.D., Jr. & Vecchi, M.P. Optimization by simulated annealing. *Science* **220**, 671-680 (1983).
16. Eydgahi, H. et al. Properties of cell death models calibrated and compared using Bayesian approaches. *Mol. Syst. Biol.* **9**, 644 (2013).
17. Stuart, K.A. et al. Hepatocyte growth factor/scatter factor-induced intracellular signalling. *Int. J. Exp. Pathol.* **81**, 17-30 (2000).
18. Viticchiè, G. & Muller, P.A.J. c-Met and Other Cell Surface Molecules: Interaction, Activation and Functional Consequences. *Biomedicines* **3**, 46-70 (2015).
19. Xu, A.M. & Huang, P.H. Receptor tyrosine kinase coactivation networks in cancer. *Cancer Res.* **70**, 3857-3860 (2010).
20. Sorkin, A. & von Zastrow, M. Endocytosis and signalling: intertwining molecular networks. *Nat. Rev. Mol. Cell Biol.* **10**, 609-622 (2009).
21. Brennan, M.D., Cheong, R. & Levchenko, A. Systems biology. How information theory handles cell signaling and uncertainty. *Science* **338**, 334-335 (2012).
22. Ferrell, J.E., Jr. Perfect and Near-Perfect Adaptation in Cell Signaling. *Cell Syst.* **2**, 62-67 (2016).
23. Goentoro, L. & Kirschner, M.W. Evidence that fold-change, and not absolute level, of beta-catenin dictates Wnt signaling. *Mol. Cell* **36**, 872-884 (2009).
24. Cohen-Saidon, C., Cohen, A.A., Sigal, A., Liron, Y. & Alon, U. Dynamics and variability of ERK2 response to EGF in individual living cells. *Mol. Cell* **36**, 885-893 (2009).
25. Lee, R.E., Walker, S.R., Savery, K., Frank, D.A. & Gaudet, S. Fold change of nuclear NF-kappaB determines TNF-induced transcription in single cells. *Mol. Cell* **53**, 867-879 (2014).
26. Shi, T. et al. Conservation of protein abundance patterns reveals the regulatory architecture of the EGFR-MAPK pathway. *Sci. Signal.* **9**, rs6 (2016).
27. Antebi, Y.E.N., N. Elowitz, M. B. An operational view of intercellular signaling pathways. *Curr. Opin. Syst. Biol.* **1**, 16-24 (2017).
28. Behar, M. & Hoffmann, A. Understanding the temporal codes of intra-cellular signals. *Curr. Opin. Genet. Dev.* **20**, 684-693 (2010).
29. Hart, Y., Mayo, A.E., Shoval, O. & Alon, U. Comparing apples and oranges: fold-change detection of multiple simultaneous inputs. *PLoS One* **8**, e57455 (2013).
30. Ferguson, S.S. Evolving concepts in G protein-coupled receptor endocytosis: the role in receptor desensitization and signaling. *Pharmacol. Rev.* **53**, 1-24 (2001).
31. Guskjolen, A.J. Losing Connections, Losing Memory: AMPA Receptor Endocytosis as a Neurobiological Mechanism of Forgetting. *J. Neurosci.* **36**, 7559-7561 (2016).

32. Carroll, R.C., Beattie, E.C., von Zastrow, M. & Malenka, R.C. Role of AMPA receptor endocytosis in synaptic plasticity. *Nat. Rev. Neurosci.* **2**, 315-324 (2001).